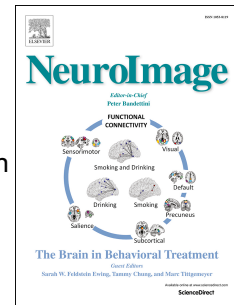


Accepted Manuscript

Somatosensory responses to nothing: An MEG study of expectations during omission of tactile stimulations

Lau M. Andersen, Daniel Lundqvist



PII: S1053-8119(18)30798-5

DOI: [10.1016/j.neuroimage.2018.09.014](https://doi.org/10.1016/j.neuroimage.2018.09.014)

Reference: YNIMG 15250

To appear in: *NeuroImage*

Received Date: 31 May 2018

Revised Date: 13 August 2018

Accepted Date: 5 September 2018

Please cite this article as: Andersen, L.M., Lundqvist, D., Somatosensory responses to nothing: An MEG study of expectations during omission of tactile stimulations, *NeuroImage* (2018), doi: 10.1016/j.neuroimage.2018.09.014.

This is a PDF file of an unedited manuscript that has been accepted for publication. As a service to our customers we are providing this early version of the manuscript. The manuscript will undergo copyediting, typesetting, and review of the resulting proof before it is published in its final form. Please note that during the production process errors may be discovered which could affect the content, and all legal disclaimers that apply to the journal pertain.

1 Somatosensory responses to nothing: an MEG study of
2 expectations during omission of tactile stimulations
3

4 Lau M. Andersen^{1*} & Daniel Lundqvist¹
5

6 ¹ NatMEG, Department of Clinical Neuroscience, Karolinska Institutet, Nobels väg 9, 171 77 Stockholm,
7 Sweden
8

9 * Corresponding author:

10 Email: lau.moller.andersen@ki.se

11 **Abstract**

12 The brain builds up expectations to future events based on the patterns of past events. This function has
13 been studied extensively in the auditory and visual domains using various oddball paradigms, but only little
14 exploration of this phenomenon has been done in the somatosensory domain. In this study, we explore how
15 expectations of somatosensory stimulations are established and expressed in neural activity as measured with
16 magnetoencephalography. Using tactile stimulations to the index finger, we compared conditions with *actual*
17 *stimulation* to conditions with *omitted stimulations*, both of which were either *expected* or *unexpected*.

18 Our results show that when a stimulation is expected but omitted, a time-locked response occurs ~135 ms
19 subsequent to the expected stimulation. This somatosensory response to “nothing” was source localized to the
20 secondary somatosensory cortex and to the insula. This provides novel evidence of the capability of the brain of
21 millisecond time-keeping of somatosensory patterns across intervals of 3000 ms.

22 Our results also show that when stimuli are repeated and expectations are established, there is associated
23 activity in the theta and beta bands. These theta and beta band expressions of expectation were localized to the
24 primary somatosensory area, inferior parietal cortex and cerebellum. Furthermore, there was gamma band activity
25 in the right insula for the first stimulation after an omission, which indicates the detection of a new stimulation
26 event after an expected pattern has been broken.

27 Finally, our results show that cerebellum play a crucial role in predicting upcoming stimulation and in
28 predicting when stimulation may begin again.

29 *Keywords:* expectations, somatosensory processing, magnetoencephalography, time-keeping, mismatch
30 responses, cerebellum

31 **1 Introduction**

32 Conceiving of the brain as not only a passive recipient of stimulation, but also as an active predictor of
33 future stimulation dates back to at least Helmholtz (1867). In support of this notion, a seminal electrophysiological
34 experiment (Näätänen et al., 1978) demonstrated that the auditory cortex generates a characteristic response to
35 deviant sounds in a sequence of otherwise standard sounds. This response, which manifested as a time-locked
36 increased negativity in the electroencephalogram (EEG) from about 130 ms to about 300 ms after stimulus onset
37 of the deviant stimuli over fronto-central electrodes, was coined the MisMatch Negativity (MMN). The MMN has
38 subsequently been explored in numerous magnetoencephalography (MEG) and EEG studies for auditory pattern
39 deviations in form of frequency, intensity, and duration shifts (Giard et al., 1995) and also in form of phonemic
40 deviations (Näätänen et al., 1997). Demonstrating the involvement of prediction in these responses, an MMN has
41 even been found when the deviant “stimulation” is in the form of a complete omission of sound, but only then if
42 the latency between sounds is briefer than ~150 ms (Yabe et al., 1997). The neural generators of the auditory
43 MMN have been localized to the primary and secondary auditory cortices (Alho, 1995).

44 MMNs have also been reported in the visual (Pazo-Alvarez et al., 2003) and somatosensory (Karhu and
45 Tesche, 1999; Tesche and Karhu, 2000) domains. Karhu and Tesche (1999) used MEG to investigate neural
46 responses to trains of median nerve stimulations applied at a 2 Hz rate with random omissions occurring 15 % of
47 the time. However, while including omissions in their stimulation sequences, these authors focussed on the
48 differences between first stimulations after an omission and the remaining stimulations, and thus did not explore
49 time-locked responses to the omissions themselves. In a follow-up study (Tesche and Karhu, 2000) however, the
50 authors reported induced cerebellar activity in the theta and gamma bands after omissions of stimuli.

51 Most researchers on this topic have studied prediction using tasks where pattern deviations are executed in
52 form of variations in the actual sensory stimulation (e.g. frequency or intensity). For researchers interested in
53 responses to violations of expectations, such stimulation variations offer a very useful approach to map out the
54 precision of the expectations and the sensitivity to violations. However, for those interested in the expectations
55 themselves, the approach contaminates the response of interest, since the neural response to a stimulation event is
56 formed by a combination of exogenous sensory stimulation, endogenous event expectations and a neural response
57 to the updating of that expectation. In our study, we aimed to separate the effects from the exogenous sensory
58 stimulation from the endogenous event expectations.

59 There has been renewed interest in the brain functions involved in expectations of somatosensory events.
60 Allen et al. (2016) using functional Magnetic Resonance Imaging (fMRI), investigated connective properties
61 between areas of the brain when stimulations unexpectedly shifted from one hand to the other. They found that the
62 thalamus, the insula, the primary somatosensory cortex (SI), middle cingulate cortex (MCC) and the middle
63 frontal gyrus (MFG) all show greater BOLD-responses for deviant stimulations than for expected stimulations.
64 Fardo et al. (2017) conducted an MEG study, also investigating the responses to stimulations unexpectedly
65 shifting from one hand to the other, and furthermore found the inferior parietal cortex (IPC) and the inferior
66 frontal gyrus (IFG) to be involved.

67 **1.1 Purpose and aims**

68 In this study, we aimed to explore how expectations of somatosensory stimulations are established and
69 expressed. For this purpose, we used regular sequences of tactile stimulations at fixed intervals that were
70 irregularly interrupted by omitted stimulations. To accomplish analysis of the neural responses to these events by
71 means of both time-locked and induced analyses, we used a long inter-stimulus interval of 3000 ms. This ISI
72 allowed us to explore expectancy responses related to the periods *before*, *at*, and *after* the point in time where
73 stimulations occurred (or should have occurred, when omitted). In terms of localizing activity related to
74 stimulations and unexpected omissions, we chose to focus on a list of *a priori* areas based on the findings of Allen
75 et al. (2016), Fardo et al. (2017) and Tesche and Karhu (2000). This included the insula, the thalamus, the middle
76 cingulate cortex (MCC), the middle frontal gyrus (MFG), the primary somatosensory cortex (SI), the inferior
77 parietal cortex (IPC), the inferior frontal gyrus (IFG) and the cerebellum. If cerebellum is involved, activity

78 should be seen ipsilaterally (Tesche and Karhu, 1997). The two hypotheses of particular interest – both targeting
79 the expression of expectations – were:

80 1) Responses to *stimulations* differ within the *a priori* areas when comparing a condition where (i) an
81 expectation has been formed to (ii) one where an expectation has *not* been formed. (Table 1: *Repeated Stimulation*
82 versus *First Stimulation*).

83 2) Responses to *no stimulation* differ within the *a priori* areas when comparing (iii) a condition where an
84 expectation has been formed with (iv) one where an expectations has *not* been formed. (Table 1: *Omitted*
85 *Stimulation* versus *Non-Stimulation*).

Table 1: Labelling of conditions as to whether stimulations and expectations are present. The labels will be further explicated in the methods section.

	Expectation	No Expectation
Stimulation	(i) <i>Repeated Stimulation</i>	(ii) <i>First Stimulation</i>
No Stimulation	(iii) <i>Omitted Stimulation</i>	(iv) <i>Non-Stimulation</i>

86 For the time-locked responses, we were mainly interested in the first two early components following
87 tactile stimulations: the contralateral SI component after ~60 ms, and the bilateral secondary somatosensory cortex
88 (SII) component after ~135 ms (Hari et al., 1984; Mima et al., 1998). For the induced responses, we were mainly
89 interested in differential activity between stimulation and omissions in the mu-bands (mu-alpha: ~8-12 Hz and
90 mu-beta: ~18-25 Hz). The theta (~4-7 Hz) and gamma (~40-100 Hz) bands were also of interest since several
91 studies have shown the involvement of these bands in encoding memories (Nyhus and Curran, 2010; Osipova et
92 al., 2006; Roux and Uhlhaas, 2014; Schack et al., 2002).

93 MEG differs in the sensitivity that it has to these areas: especially thalamic activity may be challenging to
94 localize due to its sub-cortical position (Hämäläinen et al., 1993). Insula and MCC are also in parts of the brain
95 where MEG has low sensitivity (Hillebrand and Barnes, 2002), but where localization may still be feasible. SI and
96 MFG, IFG and IPC however are cortical and thus good targets for MEG. Finally, more and more evidence is
97 surfacing for MEG being sensitive to deep sources (e.g. Attal et al., 2012; Coffey et al., 2016; Garrido et al., 2015;
98 Tenney et al., 2013), demonstrating that localization of cerebellar and thalamic activity is feasible.

99 2 Materials and methods

100 2.1 Participants

101 Twenty participants volunteered to take part in the experiment (eight males, twelve females, Mean Age:
102 28.7 y; Minimum Age: 21; Maximum Age: 47). The experiment was approved by the local ethics committee,
103 “Regionala etikprövningsnämnden i Stockholm”, in accordance with the Declaration of Helsinki.

104 2.2 Stimuli and procedure

105 Tactile stimulations were generated by using an inflatable membrane (MEG International Services Ltd.,
106 Coquitlam, Canada) fastened to the participants’ right index fingertips. The membrane was part of a custom
107 stimulation rig, and was controlled by pneumatic valves (model SYJ712M-SMU-01F-Q, SMC Corporation,
108 Tokyo, Japan) using 1 bar of pressurized air. The experimental paradigm consisted of inflating the membrane with
109 a regular interval of exactly 3000 milliseconds. At pseudo-random intervals, some of the inflations were omitted
110 such that there was a complete absence of stimulation. These omissions always happened at either the fourth, fifth
111 or sixth place in the stimulation sequence; chosen in a counterbalanced manner. An illustration of the sequence is
112 shown in Fig. 1.

113 One thousand trials were administered to each participant, of which six hundred were equally distributed as
114 *First Stimulation*, *Repeated Stimulation (2)* and *Repeated Stimulation (3)*. Two hundred were omissions, close to
115 evenly distributed between *Omitted Stimulation (4)*, *Omitted Stimulation (5)* and *Omitted Stimulation (6)*. The last

116 two hundred were distributed between *Repeated Stimulation (4)* and *Repeated Stimulation (5)*. Periods of fifteen
 117 seconds of non-stimulation were interspersed between these sequences to obtain segments of data with repeated
 118 omitted stimulation. These occurred approximately every twenty-five trials, always started after an omission, and
 119 were cued by a three-second tone. The first three seconds were a *wash-out period*, and also polluted by the tone,
 120 and thereafter four trials (3000 ms) of non-stimulation trials were segmented from the remaining twelve seconds
 121 of non-stimulation. This resulted in a total of around one-hundred-thirty epochs with no stimulation per subject
 122 (*Non-Stimulation*).

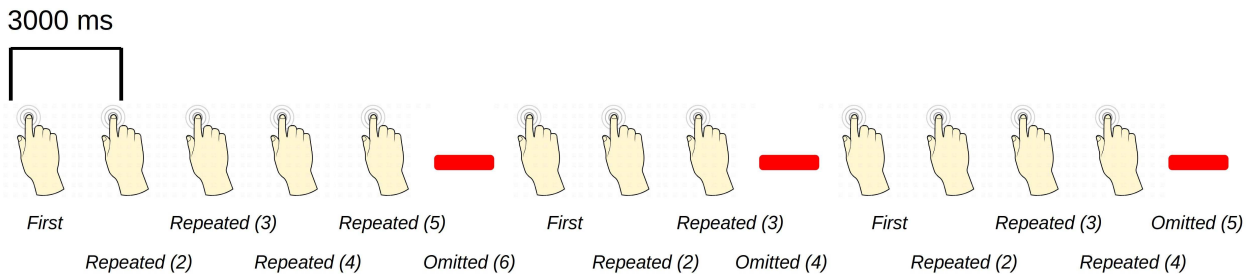


Fig. 1. Experimental paradigm: An example sequence of the experimental paradigm is shown. The annotations on the bottom show the coding used throughout for the different events of interest. Stimulations happened at a regular pace, every three seconds. When omissions occurred, there were thus six seconds between two consecutive stimulations.

123 During the stimulation procedure, participants were watching a nature programme with sound being fed
 124 through sound tubes (model ADU1c, KAR Oy, Helsinki, Finland) into the ears of participants at approximately 65
 125 dB, rendering the tactile stimulation completely inaudible. Participants were instructed to pay full attention to the
 126 movie and to pay no attention to the stimulation of their finger, which was held under a table such that it could not
 127 be seen. In this way, expectations should be mainly stimulus driven, and thus not cognitively driven or attention
 128 driven. Both before and after the administration of the one thousand trials, a period of non-stimulation lasting 3
 129 minutes was recorded. These were cut into segments of 3000 ms, resulting in 120 *No-Task* trials recorded outside
 130 the experiment. These were to be used as a common baseline activity for all four conditions (Table 1).

131 2.3 Preparation of subjects

132 In preparation for the MEG-measurement each subject had their head shape digitized using a Polhemus
 133 FASTRAK. Three fiducial points, the nasion and the left and right pre-auricular points, were digitized along with
 134 the positions of four head-position indicator coils (HPI-coils). Furthermore, about 200 extra points digitizing the
 135 head shape of each subject were acquired.

136 2.4 Acquisition of data

137 Data was recorded by an Elekta Neuromag TRIUX system inside a magnetically shielded room (model
 138 Ak3b (Vacuumschmelze GmbH) at a sampling frequency of 1000 Hz and on-line low-pass and high-pass filtered
 139 at 330 Hz and 0.1 Hz respectively.

140 2.5 Processing of MEG data

141 Two kinds of analyses were done. In the first set of analyses, we extracted responses time-locked to the
 142 onset of the actual stimulation (*Repeated* and *First Stimulation*) and to the expected onset of the *Omitted*
 143 *Stimulations*. In the second set of analyses, we extracted induced responses to the same conditions. Both kinds of
 144 analyses were also done for *Non-Stimulations*.

145 For the time-locked responses the data were first MaxFiltered (Taulu and Simola, 2006), using temporal
 146 Signal Space Separation (tSSS) with a correlation limit of 98 %, movement corrected and line-band filtered (50
 147 Hz). Subsequently the data were low-pass filtered at 70 Hz and then cut into segments of 1200 ms, 200 ms pre-
 148 stimulus and 1000 ms post-stimulus. The delay between the digital trigger and the onset of the stimulation was

149 assessed to be 41.0 ms via a separate recording using an accelerometer attached to the tactile membrane. After
150 subtracting the 41.0 ms delay, data was then demeaned using the pre-stimulus period. Segments of data including
151 magnetometer responses greater than 4 pT or gradiometer responses greater than 400 pT/m were rejected. An
152 independent component analysis was done on the segmented data to identify eye blink and heart beat related
153 components. These were subsequently removed from the segmented data. The omissions (occurring at position 4,
154 5 or 6 in a stimulation sequence) were collapsed into one response category of *Omitted Stimulations* to maximize
155 the signal-to-noise ratio.

156 For the induced responses the data were first MaxFiltered (Taulu and Simola, 2006), using tSSS with a
157 correlation limit of 98 %, movement corrected and line-band filtered (50 Hz). Subsequently, the data were then cut
158 into segments of 3000 ms, 1500 ms pre-stimulus and 1500 ms post-stimulus adjusted with the measured delay of
159 41.0 ms. Data was demeaned using the whole segment. Then data was cleaned manually by removing segments
160 showing large variance. An independent component analysis was done on the segmented data to identify eye
161 blink, eye movement and heart beat related components. These were subsequently removed from the segmented
162 data. Then, from each segment of data the respective time-locked response of the given condition was subtracted
163 from that segment. This was done to minimize the presence of time-locked responses in the induced responses.
164 Time-frequency representations were calculated from these segments of data according to condition. A Morlet
165 wavelet analysis with 7 cycles was done for frequencies from 1-40 Hz and a multitaper analysis with 5 tapers was
166 done for frequencies from 40-100 Hz. These were done for each time point from 1500 ms pre-stimulus to 1500 ms
167 post-stimulus. Data from gradiometer pairs were then combined by summing the powers from each. Finally, the
168 data were baselined by using the mean power from the *No-Task* trials. To choose which time and frequency ranges
169 to run source reconstruction on, cluster statistics on sensor-time-frequency triplets (Maris and Oostenveld, 2007)
170 was done on the differences between *Repeated* and *First Stimulation* and between *Omitted* and *Non-Stimulation*.
171 To this end, separate mass-univariate tests were run on the differences respectively between *Repeated* and *First*
172 *Stimulation* and between *Omitted* and *Non-Stimulation* with $\alpha = 0.05$. Individual time-frequency points were
173 considered to be part of a cluster if they were significant on this test *and* they had neighbouring points in space,
174 i.e. sensors, and time-frequency of the same sign, positive/negative, that were also significant. For each positive
175 and negative cluster, the *t*-values were then summed together giving a *T*-value. Subsequently, from a permutation
176 test with 2000 repetitions, labels, e.g. *Repeated* and *First*, were subsequently randomly allocated to each of the
177 conditions, giving a distribution of summed cluster values to compare against, i.e. a distribution of *T*-values.
178 Clusters were considered significant if the likelihood of the *T*-value, or of a more extreme *T*-value, of such a
179 cluster was 0.025 or smaller under the permutation distribution. This controls the false alarm rate for clusters at a
180 level of $\alpha = 0.05$. Importantly, the multiple comparisons problem is circumvented in this manner. The overall false
181 alarm rate is controlled at a level of $\alpha = 0.05$, since the null hypothesis, namely that labelling of conditions into,
182 say, *Repeated* and *First Stimulation* is not different than any other (random) labellings of conditions, is only
183 rejected if at least one negative or one positive cluster has a *T*-value that is associated with a *p*-value equal to or
184 smaller than 0.025 under the permutation distribution.

185 2.6 Source reconstruction

186 Two different strategies were followed for the source reconstruction of time-locked and induced responses
187 respectively. For the time-locked responses, a distributed solution based on the Minimum Norm Estimate (MNE)
188 (Hämäläinen and Ilmoniemi, 1994) was found, and for the induced responses a beamformer approach was used.
189 See sections below for further details. The MNE approach was chosen for the time-locked responses since it
190 provides a full-brain reconstruction with minimal assumptions about which sources are active in the cortex.
191 Oscillations have been argued to be best modelled by beamformers, however, (Hillebrand and Barnes, 2005).
192 Most of the literature pertaining source reconstructions of oscillations is also using beamformers.

193 For source reconstructing the time-locked responses, we acquired Hi-res Sagittal T1 weighted 3D IR-
194 SPGR (inversion recovery spoiled gradient echo) images for each subject using a GE MR750 3 Tesla scanner with
195 the following pulse sequence parameters: 1 mm isotropic resolution, FoV 240x240mm, acquisition matrix:
196 240x240, 180 slices, 1mm thick, bandwidth per pixel=347 Hz/pixel, Flip Angle=12 degrees, TI=400ms,

197 TE=2.4ms, TR=5.5ms resulting in a TR per slice of 1390ms. 3D gradient inhomogeneity (linearisation) correction
 198 was applied (gradwarp). Based on these images a full segmentation of the head and the brain was done using
 199 FreeSurfer (Dale et al., 1999; Fischl et al., 1999a). Based on this segmentation, the boundaries for the skin, skull
 200 and brain surfaces were found using the watershed algorithm with the MNE-C software (Gramfort et al., 2013). A
 201 source space restricting sources to the cortical sheet was created and a single compartment volume conductor
 202 model was set up based on the boundary for the brain surface, also using MNE-C. For each subject the T1 was co-
 203 registered to the subject's head shape with the fiducials and head shape points acquired with the Polhemus
 204 FASTRAK. A forward model was then made based on the transformation, the volume conductor, the source space
 205 model and the positions of the MEG sensors, (magnetometers and gradiometers). Source time courses were
 206 reconstructed using MNE (Hämäläinen and Ilmoniemi, 1994), with depth-weighting (Dale et al., 2000). The
 207 noise-estimate necessary for doing the MNE was estimated based on the pre-stimulus activity. The individual
 208 source time courses were then morphed onto a common template, the *fsaverage* (Fischl et al., 1999b), from the
 209 FreeSurfer software. Grand averages were then done over the morphed data. For statistical evaluation, 10 ms
 210 intervals were chosen around the peak times based on a combination of the literature and the observed peaks for
 211 SI and SII (56 ms and 135 ms respectively) (Hari et al., 1984; Mima et al., 1998).

212 For source reconstructing the induced responses, we used the FieldTrip software (Oostenveld et al., 2011),
 213 after applying the transformation done above, to segment the T1-images into the brain, skull and skin for each
 214 subject. From the brain segmentation a single compartment volume conductor was created. The source space was
 215 the whole brain, and was thus not restricted to the cortical sheet as in the reconstruction of the time-locked
 216 responses. A beamformer approach was used (Dynamic Imaging of Coherent Sources, DICS: Gross et al., 2001).
 217 Based on the identified components in the time-frequency representations, trial segments were cropped into time
 218 windows containing the component. From these time windows, the Fourier transforms for the frequency of
 219 interest for the *Repeated* and *First Stimulation* and the *Omitted* and *Non-Stimulation* were done. Furthermore, a
 220 Fourier transform was also done for the *No-Task* trials collected outside the experiment, to be used as a contrasting
 221 condition for all conditions (Table 1). Finally, Fourier transforms were done for the combinations of each of the
 222 conditions and the *No-Task* trials outside the experiment. Based on these Fourier transforms, sources underlying
 223 the induced responses were reconstructed with the usage of a common spatial filter estimated from the
 224 combinations of the conditions and the *No-Task* trials outside the experiment. The co-registered source space for
 225 each subject was warped onto the standard Colin-27 brain (Holmes et al., 1998). The forward model for each
 226 subject was based on the warped source space, the positions of the gradiometers and the volume conductor.
 227 Contrasts between beamformer reconstructed activity for each of the conditions (*First*, *Repeated*, *Omitted* and
 228 *Non-Stimulations*) and *No-Task* trials outside the experiment were calculated. Noise was projected out and was
 229 regularized with a lambda value set at 10% of the mean of the sum of the diagonal of the cross-spectral density
 230 matrix. These beamformer solutions revealed which regions generated the induced responses.

231 3 Results

232 Note that for all results *Repeated Stimulation* is the second stimulation (Fig. 1 and Table 1), i.e. the one
 233 following *First Stimulation*, since this is where the expectation of another stimulation can be confirmed. The
 234 reserved digital object identifier for the data repository, where data for this experiment can be freely downloaded
 235 is: 10.5281/zenodo.998518.

236 For the time-locked responses, grand averages were calculated across all participants separately for each of
 237 the conditions. The sensor space results are illustrated in Fig. 2. No statistical analyses were done in the sensor
 238 space. These were carried out in the source space.

239 *Repeated* and *First Stimulation* were compared to one another, and so were *Omitted* to *Non-Stimulation*
 240 (Table 1). The results showed that *Repeated* and *First Stimulation* were very similar with the first component
 241 occurring contralaterally to the stimulated hand at 56 ms over the somatosensory cortex (SI-component), which
 242 was followed by a second bilateral component at 135 ms over the secondary somatosensory cortices (SII-
 243 component) (Fig. 2AB). The *Omitted Stimulation* lacked the initial SI-component observed for stimulation
 244 conditions at 56 ms, but showed an SII-component at 135 ms, thus matching the timing of the second component

245 for both *Repeated* and *First Stimulation* (Fig. 2C). *Non-Stimulation* did not show any systematic components at
 246 any of these time points (Fig. 2D).

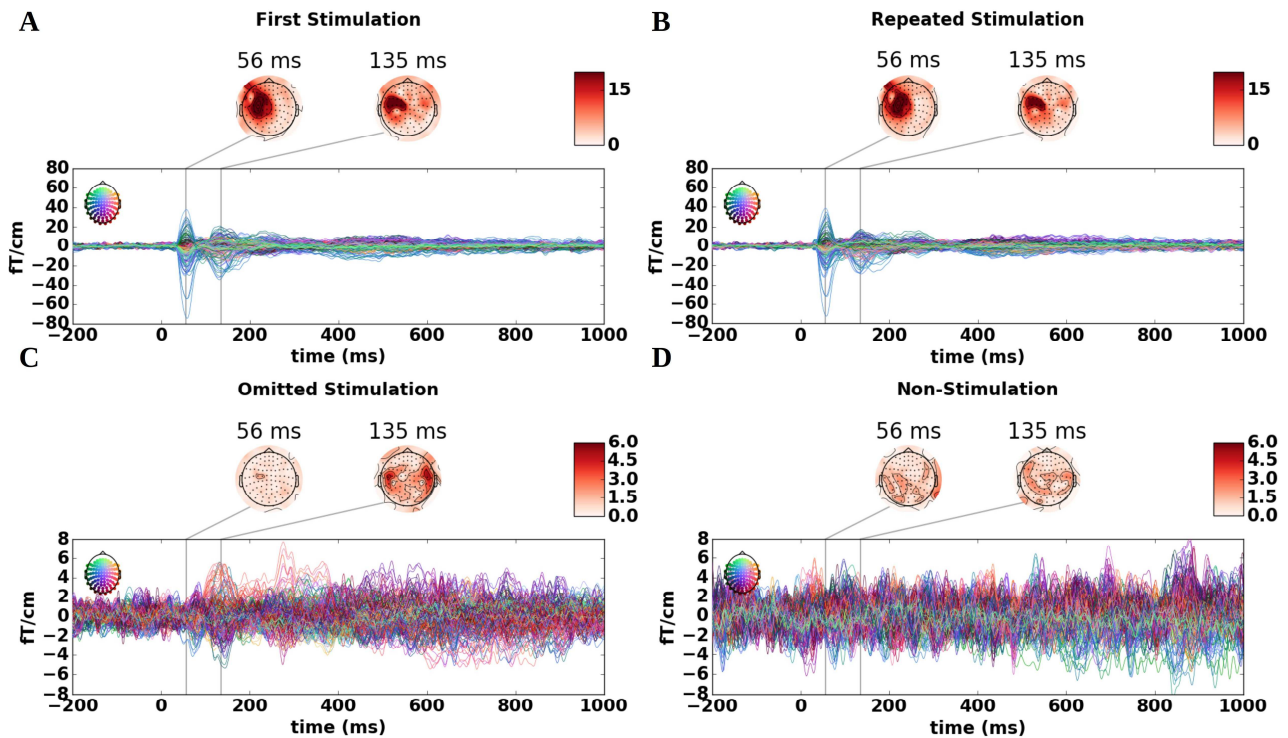


Fig. 2. Timelocked responses: Butterfly plots of the time-locked responses for the 204 gradiometers with accompanying flattened topographical plots with root mean square values of the gradiometer pairs. Coloured heads in the top-left corners of the butterfly plots indicate from which sensors data are drawn. **A)** contralateral peak for *First Stimulation* after 56 ms (SI) and bilateral peak after 135 ms (SII). **B)** similar to **A**, but for *Repeated Stimulation*. **C)** a bilateral peak after 135 ms with SII topography. **D)** For the *Non-Stimulations*, no clear components were found. Note the different scales in the top row and the bottom row.

247 The SI and SII components shown in Figs. 2A and 2B were expected after tactile stimulation, because the
 248 responses in the somatosensory cortex are known to be unfolding at a very reliable and precise pace following
 249 sensory stimulations (Hari and Forss, 1999). The time-locked responses to *Omitted Stimulation* were however
 250 more unexpected (Fig. 2C).

251 Using Minimum-Norm Estimates (as described in the methods) we reconstructed the sources for the two
 252 responses (56 ms (SI) and 135 ms (SII); see Fig. 2). To test the statistical significance of these responses, we
 253 performed permutation tests (Maris and Oostenveld, 2007) with a threshold of $\alpha = 0.05$ for the initial mass-
 254 univariate test and a subsequent cluster threshold of $\alpha = 0.025$ (Fig. 3). The data going into the test was the
 255 difference between source reconstructed time courses morphed to *fsaverage* with a 10 ms interval around the peak
 256 (i.e. 46-66 ms and 125-145 ms). Intervals were tested as described in the methods.

257 The influence from expectations on *stimulations* were explored by testing the differences between *Repeated*
 258 and *First Stimulation* for the two response components at 56 ms and 135 ms. The p -values for the biggest clusters
 259 were respectively: SI: $p = 0.58$; SII $p = 0.21$. Thus, the results showed no significant differences between
 260 *Repeated* and *First Stimulation* for any of these two response components.

261 The influence from expectations during *omissions* were explored by testing the differences between
 262 *Omitted* and *Non-Stimulations* for the same two peaks, 56 ms and 135 ms. The p -values for the biggest clusters
 263 were respectively: SI: $p = 0.58$; SII: $p = 0.0001$. Thus, the results showed a significant difference between *Omitted*
 264 and *Non-Stimulation* for the second (but not the first) response component driven by more activity in ipsilateral
 265 SII for *Omitted* compared to *Non-Stimulation*.

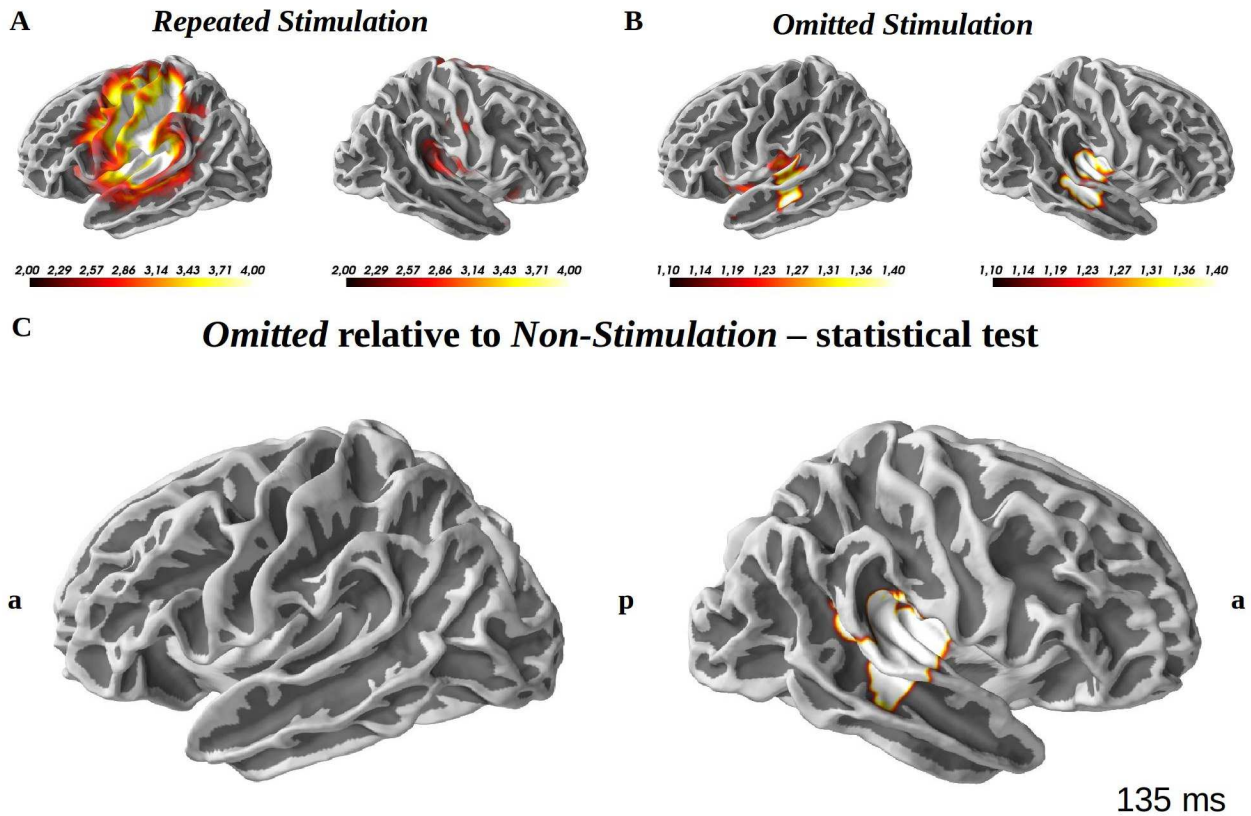


Fig. 3. Timelocked responses following repeated and omitted stimulations. Grand averages (dSPM values) for *Repeated* and *Omitted Stimulation* and a statistical map based on cluster analysis for SII-component for *Omitted* versus *Non-Stimulation* after 135 ms: **A)** grand average source activity for *Repeated Stimulation*. This revealed bilateral activation of the SII and contralateral activation of SI. **B)** grand average source activity for *Omitted Stimulation*. This revealed bilateral activation of SII. **C)** *t*-maps cluster-thresholded at 0.025 overlaid on the fsaverage brain at 135 ms. The difference response is localized to the right superior temporal gyrus, posterior insula and SII. a=anterior, p=posterior.

266 For induced responses, grand averages were calculated across all participants. Similar comparisons
 267 between conditions were made here as for the evoked responses, that is, comparing *Repeated* and *First*
 268 *Stimulation* on the one hand, and comparing *Omitted* and *Non-Stimulation* on the other. For both sets of analyses,
 269 we baselined the induced responses with the induced activity from the *No-Task* trials (segments of rest data before
 270 the task begun, but with the movie running).

271 Investigating from stimulus onset till 1000 ms post-stimulus, we found the classical responses to tactile
 272 sensory stimulation (Salmelin et al., 1995; Salmelin and Hari, 1994), which include mu-alpha (~12 Hz) and mu-
 273 beta (~22 Hz) suppression from 150 ms to 500 ms and a mu-beta (~18 Hz) rebound from 500 ms to 900 ms (Fig.
 274 4). Furthermore, a theta synchronization (~7 Hz) from -100 ms to 350 ms was found for both *Repeated* and *First*
 275 *Stimulation*, but with seemingly greater power for *Repeated* than for *First Stimulation* (Fig. 4B). For *Omitted* and
 276 *Non-Stimulation* these components were not clearly found (Fig. 4B).

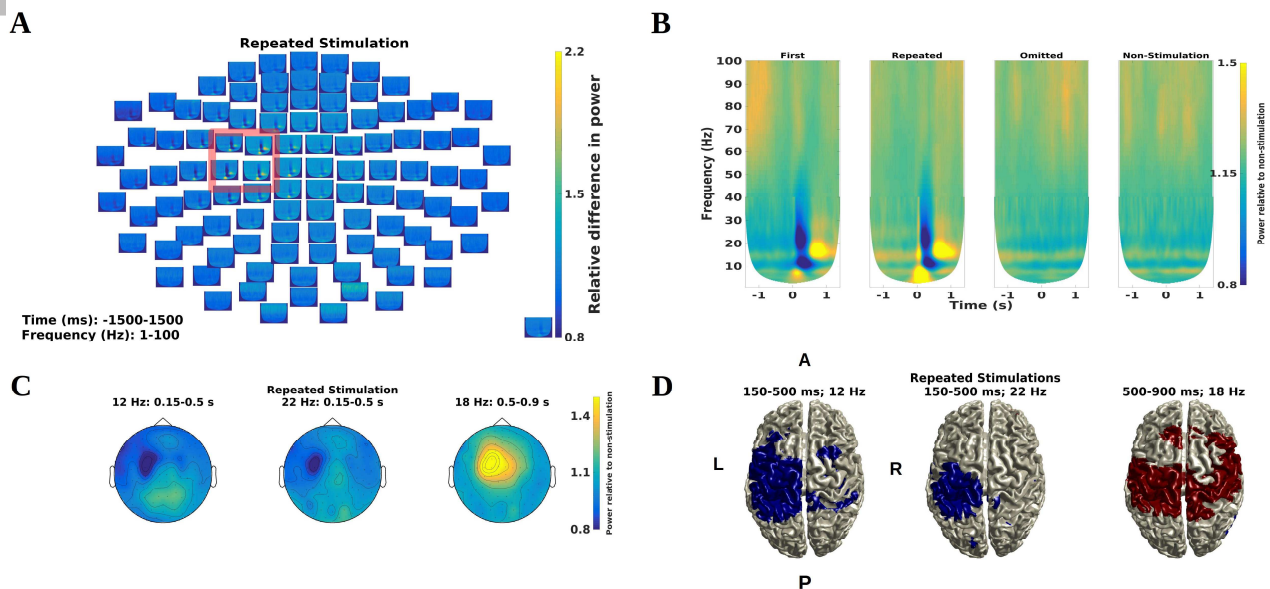
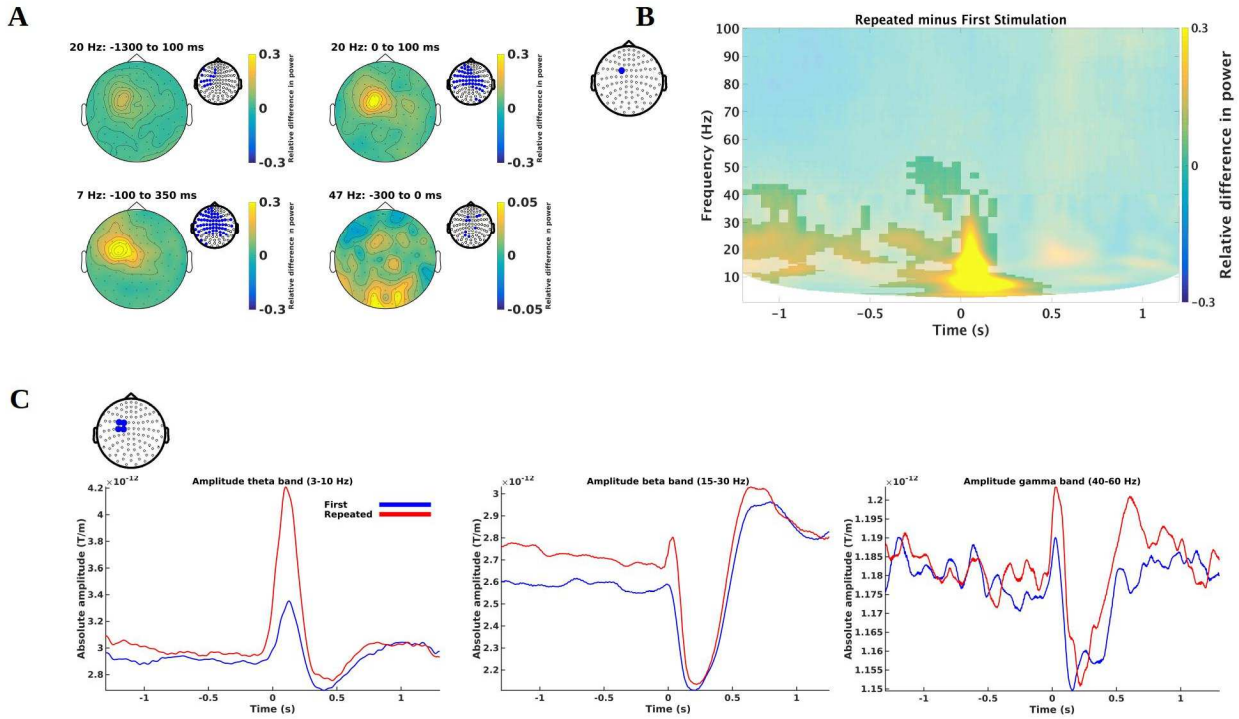


Fig. 4. Induced responses during stimulation and during the absence of stimulation: Grand average time-frequency representations for gradiometer pairs. **A)** *Repeated Stimulation* channel plots. **B)** Mean of channels in the red square in **A)** for all conditions (Table 1): both the mu-alpha and mu-beta bands suppressions and the mu-beta rebound are seen for the stimulations, but not for the absence of stimulation. **C)** Topographical plots for *Repeated Stimulation*, showing a contralateral topography for all alpha and beta synchronizations and desynchronizations. **D)** Beamformer surface source reconstructions of the activity underlying the topographical plots, with activity significant at an alpha level of 0.05 (Red is greater than zero, blue is lesser than zero). For all plots, power is relative to the power for the *No-Task* trials recorded outside the experiment.

277 The influence from expectations during stimulations were explored by testing the differences between
 278 *Repeated* and *First Stimulation*. This comparison revealed higher power for *Repeated* than for *First Stimulation* in
 279 the theta, beta and gamma bands (Fig. 5). The theta band increase was before and after the stimulation (~7 Hz;
 280 from -100 ms to 350 ms). A beta band increase followed the stimulation directly (~20 Hz; from 0 ms to 100 ms).
 281 It is not likely that these differences were related to phase-locked activity since no differences were found between
 282 *Repeated* and *First Stimulation* in the time-locked responses (Fig. 2AB). The gamma band increase was found in
 283 the pre-stimulus time period (-300 ms to 0 ms at ~47 Hz). Finally, the beta band showed increased activity pre-
 284 stimulus (~20 Hz; from -1300 ms to 0 ms). These four increases in synchronization were all identified in the
 285 biggest cluster ($p < 0.001$) when testing the differences between *Repeated* and *First Stimulation* (Fig. 5B).

286 Since it is potentially possible that the theta, beta and gamma band increases for *Repeated* relative to *First*
 287 *Stimulation* are simply due to refractory activity from the preceding stimulation, we examined this possibility by
 288 calculating the temporal spectral evolution of these frequency bands (Salmelin and Hari, 1994) (Fig. 5E). We
 289 demeaned the resulting time courses by taking the mean of the activity from -1300 ms to -500 ms to ensure that
 290 any differences found were not consequences of offset differences. We then tested using cluster statistics whether
 291 these peaks for *Repeated Stimulation* were significantly higher than the corresponding peaks for *First Stimulation*.
 292 The results showed that the increases in power for *Repeated* compared to *First Stimulation* (Fig. 5) were
 293 statistically significant for the theta, $p < 0.001$, and the beta bands, $p = 0.0015$, but not for the gamma band, $p =$
 294 0.0575 . The clusters, respectively, for the theta and the beta bands, extended from 19 ms to 232 ms and from 15
 295 ms to 92 ms, closely matching the periods found in the induced responses. This indicates that the increases in
 296 induced responses found for *Repeated* relative to *First Stimulation* cannot be explained simply by increased
 297 activity due to the preceding stimulation.



298

Fig. 5. Differences in induced responses due to differences in expectations during stimulation: Differences between *Repeated* and *First Stimulation*. **A)** Topographical plots of theta, beta and gamma band differences. Channels that are part of the cluster found in the permutation test are indicated by the blue dots on the channel topographies next to the difference plots. Clusters shown are for the time point in between the two time points and the frequency in the respective titles. **B)** Plot of a single channel showing the theta, beta and gamma band differences. Differences associated with a cluster with a p -value lower than an alpha of 0.025 are shown non-blurred. The position of the channel shown is indicated by the blue dot on the topography. **C)** Temporal spectral evolution plots of the theta, beta and gamma bands. These are based on an average of the four channels indicated by the blue dots on the topography.

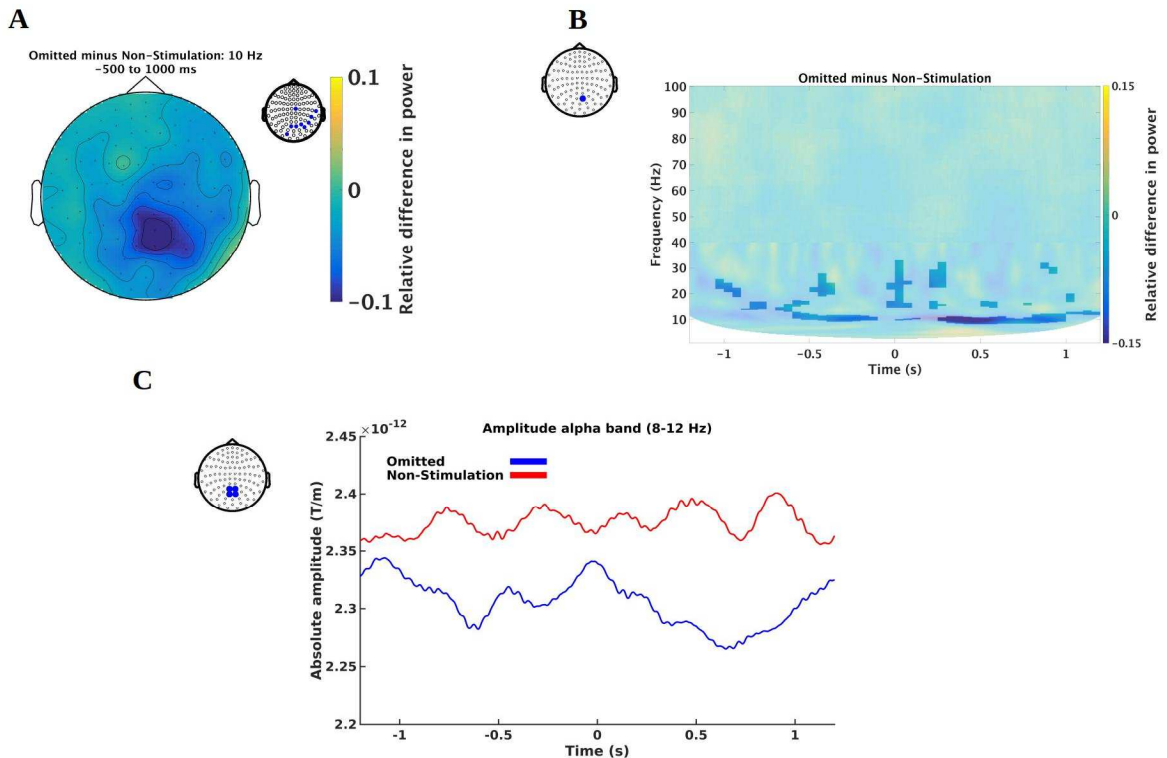


Fig. 6. Differences in induced responses due to differences in expectations during during the absence of stimulation: Differences between *Omitted* and *Non-Stimulations*. **A)** Lower power in the alpha band (10 Hz) for *Omitted* relative to *Non-Stimulation*. Channels that are part of the cluster found in the permutation test are indicated by the blue dots on the channel topography next to the difference plot. The cluster shown is for the time point in between the two time points and the frequency in the title. **B)** Plot of a single channel showing an alpha band difference. Differences associated with a cluster with a p -value lower than an alpha of 0.025 are shown non-blurred. The position of the channel shown is indicated by the blue dot on the topography. **C)** Temporal spectral evolution plots of the alpha band. The lines are based on an average of the four channels indicated by the blue dots on the topography.

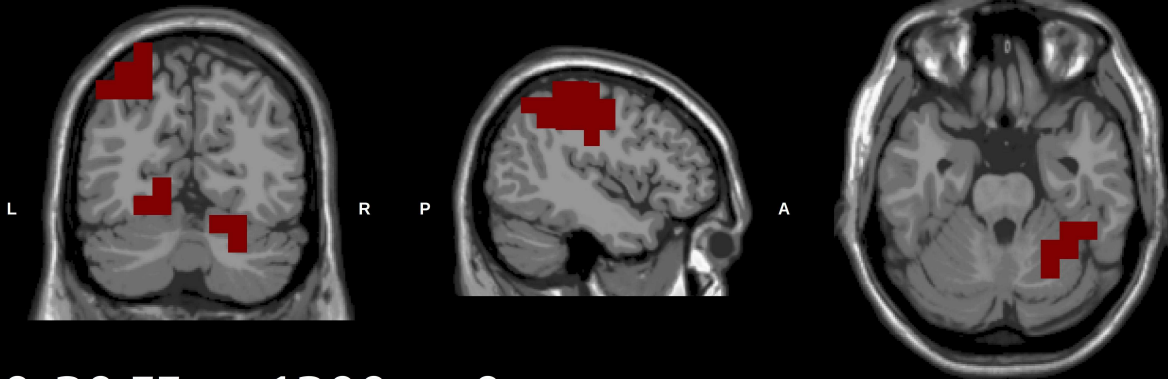
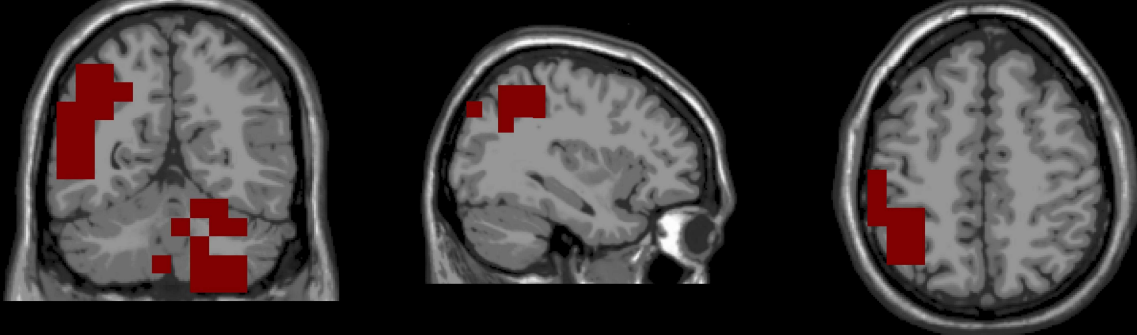
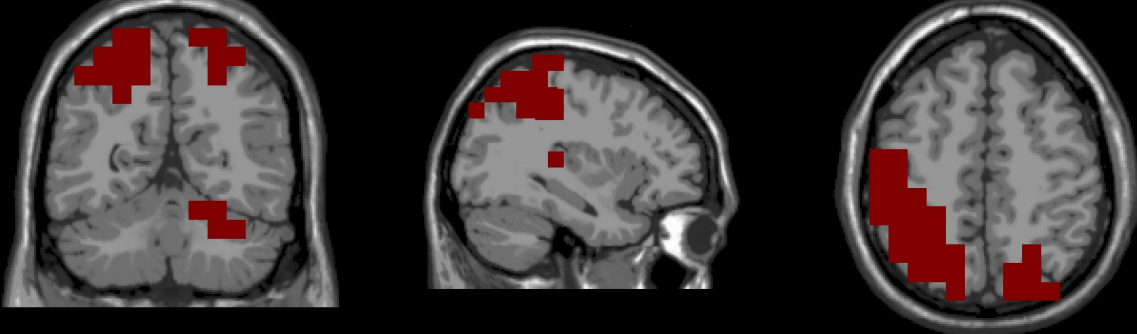
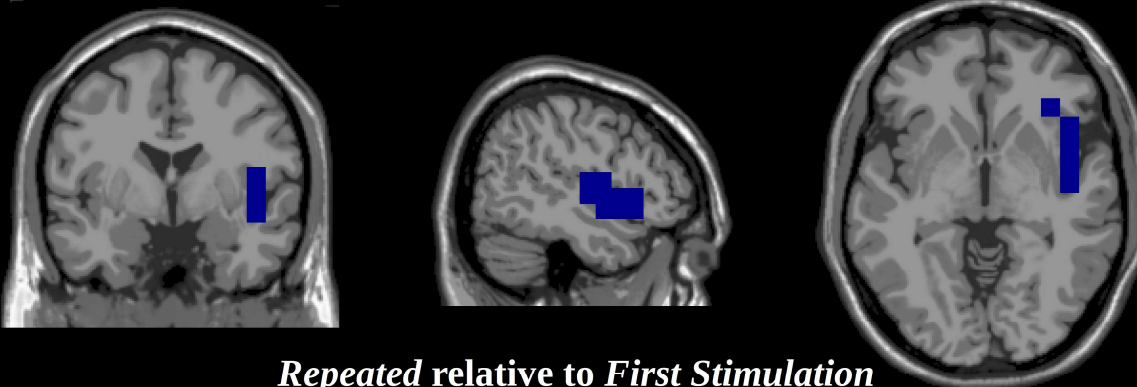
299 The influence from expectations during stimulations were explored by testing the differences between
 300 *Omitted* and *Non-Stimulation*. This comparison revealed lower power for *Omitted Stimulation* than for *Non-*
 301 *Stimulation* in the alpha band (Fig. 6). The decrease was found both before and after time point of the omitted
 302 stimulation (~10 Hz; from -500 ms to 1000 ms). This decrease in synchronization was identified in the biggest
 303 cluster ($p < 0.001$) when testing the differences between *Non-Stimulation* and *Omitted Stimulation* (Fig. 6B).

304 The above results from the analysis of induced responses were followed up with source space analyses
 305 below. We performed beamformer source reconstructions for the alpha, beta, theta and gamma bands activity
 306 using the methods described in the methods section. Statistical tests for the *a priori* areas of interest (insula,
 307 thalamus, MCC, MFG, SI, IPC, IFG and cerebellum) were extracted below. For each of the areas the maximum
 308 unsigned value was extracted from each subject for that parcellation according to the AAL-atlas (Tzourio-
 309 Mazoyer et al., 2002). The statistical within-subject, between-conditions testing was done based on these values
 310 (Figs. 7-8 and Tables 2-3). No corrections for multiple comparisons were done on the beamformer reconstructions
 311 since the alpha level had already been controlled at $\alpha = 0.05$ by the earlier permutation test (i.e. had there been no
 312 significant effect of the permutation test, no beamformer reconstructions would have been done). Note that the
 313 IFG in this study is defined as Brodmann Area 44, based on the coordinates supplied in Fardo et al. (2017).

314 The activity related to the mu-alpha band (12 Hz, from 150 ms to 500 ms) and to the mu-beta band (22 Hz,
 315 from 150 ms to 500 ms; and from 500 ms to 900 ms, 18 Hz) were localized to the contralateral somatosensory and
 316 motor cortices (see Fig. 4D).

317 These source localizations replicate what has been reported in the literature for induced responses of tactile
 318 stimulation before (Cheyne, 2013) and thus serve as a sanity check that our stimulation worked as intended. Since
 319 no differences were found between *Repeated* and *First Stimulation* in the induced responses for these bands, no
 320 statistical comparisons were made. Note that no parcellation was used for these alpha and beta bands analyses,
 321 since these only served as sanity checks.

322 The role of expectations during stimulation was tested by contrasting *Repeated* against *First Stimulation*.
 323 All three bands, theta, beta and gamma, showed greater power over contralateral SI and IPC for *Repeated* as
 324 compared to *First Stimulations* (Fig. 7). The SI activity was however absent during the pre-stimulus period, -1300
 325 to 0 ms. Also for *Repeated* contrasted to *First Stimulations*, the theta and beta bands showed greater power over
 326 the right cerebellum (Fig. 7). The theta and beta bands revealed very similar patterns of activations. Finally, for
 327 *First* contrasted against *Repeated Stimulations* greater activation in the gamma band was found in the right insula
 328 (Fig. 7).

3-10 Hz: -100 to 350 ms**10-30 Hz: -1300 to 0 ms****10-30 Hz: 0 to 100 ms****40-60 Hz: -300 to 0 ms**

Repeated relative to First Stimulation

Fig. 7. Statistical t -maps of areas showing significant power differences based on beamformer reconstructions of stimulations: Both the theta and beta bands showed more activity for *Repeated* than for *First Stimulations* in the right-lateralized cerebellum and in the left inferior parietal cortex. SI, however, only showed increased activity at the times around stimulation. The gamma band showed greater activity for *First* than for *Repeated Stimulation*. **Red:** significantly greater activity for *Repeated* compared to *First Stimulation*. **Blue:** significantly

greater activity for *Repeated* compared to *First Stimulation*. An alpha threshold of 0.05 is used. Tests are run across parcellations based on the AAL-atlas. Axis keys: L=Left, R=Right, A=Anterior, P=Posterior. The slices viewed are respectively: $x_1 = -44$ mm, $y_1 = -65$ mm, $z_1 = -26$ mm; $x_2 = -35$ mm, $y_2 = -57$ mm, $z_2 = 48$ mm; $x_3 = -35$ mm, $y_3 = -57$ mm, $z_3 = 48$ mm; $x_4 = 48$ mm, $y_4 = -1$ mm, $z_4 = -4$ mm, all in MNI space.

Brain Region	7 Hz (3-10 Hz) from -100 to 350 ms		20 Hz (16-30 Hz) from -1300 ms to 0 ms		20 Hz (16-30 Hz) from 0 ms to 100 ms		47 Hz (38-54 Hz) from -300 ms to 0 ms	
	Left	Right	Left	Right	Left	Right	Left	Right
<i>Insula</i>	$t = -0.0006$ $p > 0.05$	$t = -0.407$ $p > 0.05$	$t = 0.145$ $p > 0.05$	$t = 1.50$ $p > 0.05$	$t = 1.88$ $p > 0.05$	$t = -0.186$ $p > 0.05$	$t = -0.606$ $p > 0.05$	$t = -2.44$ $p < 0.05$
<i>Thalamus</i>	$t = 1.33$ $p > 0.05$	$t = 0.384$ $p > 0.05$	$t = 1.14$ $p > 0.05$	$t = 1.02$ $p > 0.05$	$t = 1.20$ $p > 0.05$	$t = -0.333$ $p > 0.05$	$t = -0.315$ $p > 0.05$	$t = 0.0078$ $p > 0.05$
<i>MCC</i>	$t = 1.42$ $p > 0.05$	$t = 0.73$ $p > 0.05$	$t = 0.128$ $p > 0.05$	$t = 0.242$ $p > 0.05$	$t = 1.33$ $p > 0.05$	$t = 0.460$ $p > 0.05$	$t = -0.282$ $p > 0.05$	$t = -0.408$ $p > 0.05$
<i>MFG</i>	$t = 1.09$ $p > 0.05$	$t = -1.10$ $p > 0.05$	$t = -0.864$ $p > 0.05$	$t = 1.28$ $p > 0.05$	$t = 0.549$ $p > 0.05$	$t = -0.939$ $p > 0.05$	$t = 0.660$ $p > 0.05$	$t = 0.568$ $p > 0.05$
<i>SI</i>	$t = 2.19$ $p < 0.05$	$t = -0.600$ $p > 0.05$	$t = -0.161$ $p < 0.01$	$t = -0.0893$ $p > 0.05$	$t = 3.33$ $p < 0.01$	$t = 0.631$ $p > 0.05$	$t = -0.913$ $p > 0.05$	$t = 0.0106$ $p > 0.05$
<i>IPC</i>	$t = 2.17$ $p < 0.05$	$t = -0.917$ $p > 0.05$	$t = 2.24$ $p < 0.05$	$t = 1.25$ $p > 0.05$	$t = 3.24$ $p < 0.01$	$t = 0.839$ $p > 0.05$	$t = 0.153$ $p > 0.05$	$t = -0.0950$ $p > 0.05$
<i>IFG</i>	$t = -0.302$ $p > 0.05$	$t = 0.952$ $p > 0.05$	$t = -1.12$ $p > 0.05$	$t = 0.911$ $p > 0.05$	$t = 1.56$ $p > 0.05$	$t = 0.518$ $p > 0.05$	$t = -0.107$ $p > 0.05$	$t = -1.20$ $p > 0.05$
<i>Cerebellum 6</i>	$t = -0.0821$ $p > 0.05$	$t = 2.16$ $p < 0.05$	$t = 1.26$ $p > 0.05$	$t = 2.72$ $p < 0.05$	$t = 1.57$ $p > 0.05$	$t = 2.41$ $p < 0.05$	$t = -0.0218$ $p > 0.05$	$t = -0.541$ $p > 0.05$

Table 2. Tests of expectations during stimulation for the a priori areas: Statistical tests for stimulation main effects ($df = 19$) for areas reported by Allen et al. (2016), Fardo et al. (2017) and the cerebellum (Tesche and Karhu, 2000). **Red:** significantly greater activity for *Repeated* compared to *First Stimulation*. **Blue:** significantly greater activity for *Repeated* compared to *First Stimulation*. An alpha threshold of 0.05 is used.

329 The role of expectations during absence of stimulation was tested by contrasting *Omitted* to *Non-*
330 *Stimulation*. For this contrast, the alpha band revealed greater synchronization in the right cerebellum (Fig. 8) for
331 *Non-Stimulation* compared to *Omitted*. See Table 3 for a summary of all the a priori areas.

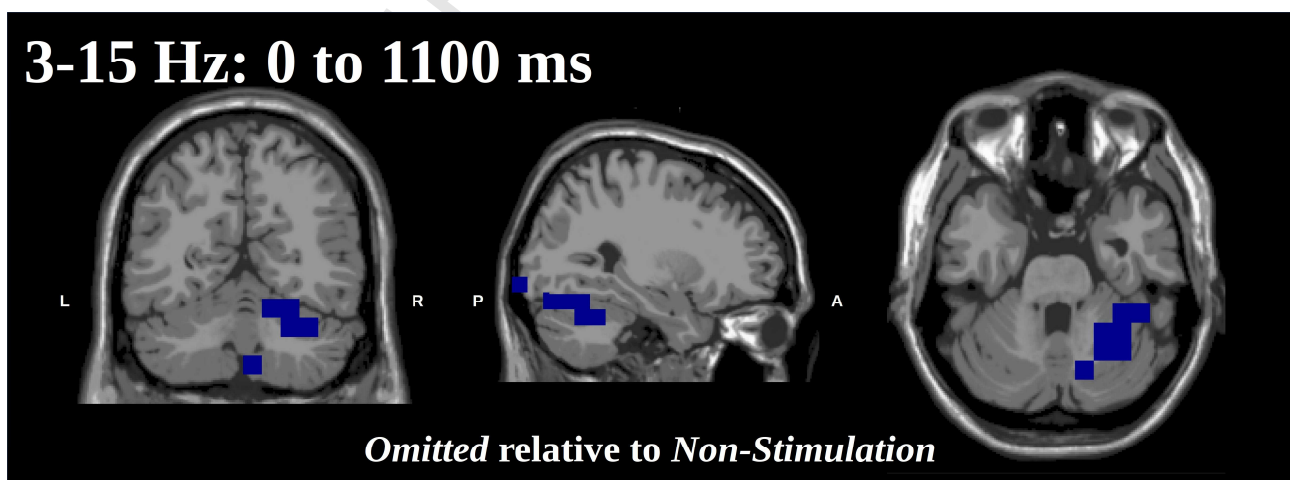


Fig. 8. Statistical t-maps of areas showing significant power differences based on beamformer reconstructions of stimulations: The alpha band showed less activity for *Omitted* than for *Non-Stimulation* in the right-lateralized cerebellum. **Blue:** significantly greater activity for *Non-Stimulation* compared to *Omitted*. An alpha threshold of 0.05 is used. Tests are run across parcellations based on the AAL-atlas. Axis keys: L=Left, R=Right, A=Anterior,

P=Posterior. The slices viewed are: $x_1 = 28$ mm, $y_1 = -59$ mm, $z_1 = -29$ mm in MNI space.

Brain Region	10 Hz from 0 ms to 1110 ms	
	Left	Right
<i>Insula</i>	$t = -0.513$ $p > 0.05$	$t = 0.193$ $p > 0.05$
<i>Thalamus</i>	$t = 0.0581$ $p > 0.05$	$t = -2.01$ $p > 0.05$
<i>MCC</i>	$t = -0.945$ $p > 0.05$	$t = -1.02$ $p > 0.05$
<i>MFG</i>	$t = 1.62$ $p > 0.05$	$t = 1.36$ $p > 0.05$
<i>SI</i>	$t = 0.260$ $p > 0.05$	$t = -1.40$ $p > 0.05$
<i>IPC</i>	$t = -0.210$ $p > 0.05$	$t = -1.87$ $p > 0.05$
<i>IFG</i>	$t = 0.768$ $p > 0.05$	$t = -0.256$ $p > 0.05$
<i>Cerebellum 6</i>	$t = 0.921$ $p > 0.05$	$t = -2.42$ $p < 0.05$

Table 3. Test of expectations during absence of stimulation for the *a priori* areas: Statistical tests for stimulation main effects ($df = 19$) for areas reported by Allen et al. (2016), Fardo et al. (2017) and the cerebellum (Fardo et al., 2017) (Tesche and Karhu, 2000). **Blue:** significantly greater activity for *Non-Stimulation* compared to *Omitted*. An alpha threshold of 0.05 is used.

332 4 Discussion

333 In this study, we explored how expectations of somatosensory stimulations are established and expressed in
334 neural response patterns as measured with MEG. Using experimental conditions with actual stimulation and
335 omitted stimulations, both of which were either expected or unexpected, we aimed at elucidating the expression of
336 expectations both during stimulations and during omissions.

337 4.1 A precisely time- and phase-locked manifestation of expectation

338 As an initial data quality control, we observed the “classical” responses subsequent to all our actual
339 stimulation events, both in terms of time-locked responses (Fig. 2AB) and induced responses in the time-
340 frequency domain (Fig. 4). The time-locked responses hence displayed the typical somatosensory SI (~60 ms) and
341 SII (~135 ms) components (Hari and Forss, 1999); and the induced responses displayed the expected mu-alpha
342 and mu-beta patterns with desynchronization at ~12 and ~22 Hz from 150 ms to 500 ms and a beta rebound at ~18
343 Hz from 500 ms to 900 ms (Fig. 4CD) (Salmelin et al., 1995; Salmelin and Hari, 1994).

344 Our study also provide new findings: When a stimulation is expected but omitted, there is a time-locked SII
345 and right insular response occurring at ~135 ms subsequent to the expected stimulation (Fig. 3). These results
346 revealed a precisely time- and phase-locked response following the expected onset of an *Omitted Stimulation*,
347 despite an inter-stimulus interval of 3000 ms (Fig. 2C), and thus provide novel evidence of the capability of the
348 brain for doing very precise time-keeping of expected events across extended intervals. This finding is particularly
349 surprising, considering related results from the auditory modality, where time-locked responses to omitted
350 stimulations have only been demonstrated when the inter-stimulus interval is twenty times shorter (less than 150
351 ms) (Yabe et al., 1997). The difference in time-keeping across inter-stimulus intervals between the auditory and
352 somatosensory systems might be due to the differences between the quality of auditory stimuli (such as speech
353 and environmental sounds), which typically are brief and abrupt, and the quality of tactile stimuli, which are often
354 comparatively slow and prolonged. Note however that a recent study of Naeije et al. (2018) did not find any
355 evidence for timelocked activity related to omitted somatosensory stimulations when the inter-stimulus interval

356 was 500 ms event though their source reconstructions also localized the source to SII. The disagreement between
357 their results and our present results indicate that longer inter-stimulus interval than 500 ms 3000 ms may be
358 necessary to generate SII responses of a sufficient amplitude for identification.

359 4.2 Theta, beta, and gamma increases after expected stimulations

360 Our study also shows that when comparing *Repeated Stimulation* to *First Stimulation*, and hence isolating
361 the influence of expectations during stimulations, there is an increase in theta band synchronization (~7 Hz, from -
362 150 ms to 350 ms) and beta band synchronization (~20 Hz, from 0 ms to 100 ms) associated with expectation
363 (Fig. 5). For these two increases in synchronization, beamforming revealed increased activity in *Repeated* relative
364 to *First Stimulation* in somatosensory, parietal and cerebellar sources (Fig. 7 & Table 2). Leading up to the
365 stimulation, we also found increased beta (~20 Hz, from -1300 ms to 0 ms) and gamma band synchronization
366 (~47 Hz, from -300 ms to 0 ms) (Fig. 5). For the increase in beta band synchronization before stimulation,
367 beamforming revealed parietal and cerebellar sources, but no somatosensory sources. This indicates that
368 stimulations are followed by refractory activity in the inferior parietal cortex and the cerebellum and that these
369 synchronizations result in the increase in synchronization of SI theta and beta band activity (Allen et al., 2016). A
370 similar role of inferior parietal cortex has also been reported by Fardo et al. (2017), where results from
371 localizations of event-related fields from a tactile oddball indicated that inferior parietal cortex was involved in
372 updating expectations.

373 One could possibly argue that the differences in theta and beta between *Repeated and First Stimulation*
374 (Figs. 5 & 7 & Table 2) could simply be interpreted as gating activity, (Arnfred et al., 2001; Swerdlow et al.,
375 1992), attenuating the magnitude of the subsequent, and expected stimulations. If this was the case, the observed
376 increase in power would reflect increased inhibition of the processing of such expected stimulations. Two things
377 however speak against such an interpretation. First, no habituation effects were observed on the evoked fields
378 (Fig. 2), while habituation has been reported in studies with shorter inter-stimulus intervals (< 2 s) (Cheng et al.,
379 2017; Hsiao et al., 2013). Second, conversely to what was found here, the influence from gating on beta
380 oscillations have been shown to show *higher* synchronization for the first than for the second stimulation when
381 stimulations are presented in pairs (Hsiao et al., 2013). The increase in theta and beta power between *Repeated*
382 and *First Stimulation* in our results hence appears to be a true manifestation of expectation rather than a gating
383 phenomenon.

384 Another interpretation of the observed increase in beta power between *Repeated Stimulations* and *First*
385 *Stimulation* is that the beta band would be signalling the status quo as according to Engel and Fries (2010). An
386 intuitive conception of what the status quo amounts to is exemplified by idling rhythms, e.g. the mu-rhythm over
387 central sensors and the alpha rhythm over posterior sensors, when the subject is at rest (Niedermeyer and Silva,
388 2005). Engel and Fries, however, extended the idea for status quo from an idling rhythm (Pfurtscheller et al.,
389 1996) to also include the perceptual set, the sensory expectations, where they hypothesize that maintenance of the
390 sensory expectation would cause increased synchronization in the beta band. Such an increase may hence be what
391 we see in the beta band change at stimulation, 0 to 100 ms, (Figs. 5 & 7) from *First Stimulation*, where no sensory
392 expectation is yet established, to *Repeated Stimulation*, where the sensory expectation is established and needs to
393 be maintained, which the present results would indicate would be done by inferior parietal cortex and cerebellum
394 (-1300 ms to 0 ms) (Fig. 7 & Table 2).

395 The present results may seem to be in opposition to earlier results where expected and attended tactile
396 stimuli were accompanied by desynchronizations in the beta band (van Ede et al., 2011, 2010). These previous
397 experiments, however included an *active* task for the participants, contrary to the current experimental *passive*
398 protocol. This means that that in those previous studies, the tactile stimulations must be processed attentively for
399 the research participant to perform the task at an acceptable level. In the current study, no tasks were involved, and
400 hence no such attentive or otherwise active processing was necessary. Rather, subjects were engaged with looking
401 at a documentary movie and if anything directing their attention away from the tactile stimulations.

402 The gamma differences were wholly related to less activity for *Repeated* relative to *First Stimulation*
403 activity in the right insula, an area which has been reported to be related to anticipation for the consequences of
404 touch (Lovero et al., 2009) and coordinating activity related to prediction errors regarding upcoming stimulation
405 (Allen et al., 2016). The gamma-band activity likely serves the purpose of updating the internal state in the
406 network, with right insula signalling that a new chain of stimulations has begun (Allen et al., 2016) (Fig. 7 &
407 Table 2).

408 Neither the thalamus, the MCC nor the frontal gyri – all included among the *a priori* areas – showed any
409 differences between the conditions. However, both the thalamus and the MCC are in areas where MEG shows
410 little sensitivity (Hillebrand and Barnes, 2002), and hence the present study might be underpowered to find them.
411 Also, in the study of Fardo et al. (2017) the IFG showed effects relative to attention and not directly to
412 expectation.

413 Between *Non-Stimulations and Omitted Stimulations* – reflecting the role of expectations in the absence of
414 stimulations – we found a difference in the alpha band (~10 Hz, from 0 ms to 1100 ms) (Fig. 6). This comparison
415 revealed lower power in the right cerebellum for *Omitted Stimulations* compared to *Non-Stimulations*. The activity
416 difference does not emerge as related to the expected onset of the *Omitted Stimulation*, but rather as a continuing
417 desynchronization, as compared to *Non-Stimulation* (Fig. 6D). At this moment, it is not entirely clear what this
418 represents.

419 **4.3 Role of cerebellum and parietal cortex – maintaining the status quo?**

420 Our results also showed power differences in the right cerebellum for the theta and beta bands, with more
421 activation for *Repeated* than *First Stimulation* (Figs. 7-8 and Tables 2-3). The refractory activity in the beta band
422 after a stimulation (Fig. 5) was found in left inferior parietal cortex and the right cerebellum.

423 A tentative interpretation of this is that during tactile stimulation, *First Stimulation*, activates continuing
424 cerebellar and parietal responses and that each new stimulation, *Repeated Stimulation*, is accompanied by stronger
425 SI activation at stimulation due to these continuing cerebellar and parietal activities. In this sense, the refractory
426 cerebellar activity and inferior parietal cortex in the beta band may be responsible for maintaining the status quo
427 (Engel and Fries, 2010). To strengthen this interpretation, it would however be necessary to find dissociative
428 evidence, such as cases where there is no beta band peak at the time of stimulation (as in Fig. 5E) even though the
429 stimulation is a repetition. From the earlier literature (Tesche and Karhu, 2000), it has been suggested that the
430 cerebellar activity has a refractory period of 2-4 s. Future studies could therefore aim at varying the inter-stimulus
431 interval and including intervals beyond this refractory period. Given the refractory period of 2-4 s for cerebellar
432 activity, it would furthermore be interesting to investigate how dependent the time-locked effect is on the duration
433 between stimulations, within and outside the 2-4 second time window. Indeed, the results of Naeije et al. (2018)
434 indicate that there might also be a lower limit on when this effect can be detected, as indicated by the absence of a
435 significant effect for omitted stimuli when the inter-stimulus interval was 500 ms.

436 One thing that one must always consider in MEG studies is how much credibility one is willing to assign to
437 subcortical localizations. The cerebellum gains credibility by having been detected in earlier studies (Tesche and
438 Karhu, 2000) and also from the theoretical knowledge that cerebellum is activated ipsilaterally to stimulation, as
439 was also found in the current study (Fig. 10). Also more and more studies are surfacing for MEG being sensitive
440 to deep sources (Attal et al., 2012; Coffey et al., 2016; Garrido et al., 2015; Tenney et al., 2013; Tesche and Karhu,
441 1997). The sensitivity to deep sources is also dependent on the MEG sensors used, with magnetometers being
442 more sensitive to deep sources than gradiometers, be they planar or axial. For future work, it would be of great
443 value to have more detailed models for the cerebellum such that the orientations and positions of potential sources
444 can be modelled with greater accuracy and thus subsequently raise our belief in subcortical localizations.

445 To explore the consistency of the cerebellar localizations, different lambda values were tested to see the
446 impact of regularization (Supplementary Material). Lambda values based on 15, 20, 30, 40, 50, 75 and 100% of
447 the mean of the sum of the diagonal of the cross-spectral density matrix were explored. For the theta band (~7 Hz

448 from -100 to 350 ms) and the beta band (~20 Hz, from 0 to 100 ms), Cerebellum 6 was found consistently. For the
 449 beta band (~20 Hz, from -1300 to 0 ms), Cerebellum 6 was found less consistently with activity being
 450 reconstructed closer to the Vermis, as also found by Tesche and Karhu (2000). Finally, for the alpha band (~10 Hz,
 451 from 0 to 1100 ms), the reconstructions moved more toward Cerebellum 9. These results show that the cerebellar
 452 results are robust, but that finer cerebellar models and advanced method will advance the precision we can hope to
 453 obtain for MEG of the cerebellum.

454 Finally, it should be mentioned that understanding the formation and resilience of expectations may also be
 455 important for understanding clinical conditions such as schizophrenia and psychosis where patients' perceptions
 456 are often (wrongfully) biased by their expectations (Aleman et al., 2003; Teufel, 2018). The present paradigm may
 457 be a valuable tool for exploring these facets.

458 **5 Conclusions**

459 This study aimed at elucidating the expression of expectations both during actual tactile stimulations and
 460 during omitted stimulations. The results provide new insights into how the brain updates and maintains the
 461 expectations towards sensory touch. We show that neural processing of omissions occurs in a precisely time-
 462 locked manner, and that it is generated by posterior insula and SII for the time-locked responses. This indicates
 463 that the brain keeps a very precise timing of when events are expected to happen even across intervals of 3000 ms,
 464 well beyond what has been earlier reported in the literature. We also show that gamma band activity is involved in
 465 updating the brain about new stimulations. In this way the insula plays a dual role, showing activity that correlates
 466 both with omitted stimulations and with the first stimulation of new chains of stimulation.

467 Refractory beta band activity was found in the cerebellum and the inferior parietal cortex after a
 468 stimulation. Extra involvement of SI when stimulations were repeated was also found. This may be interpreted as
 469 the beta band signalling the status quo – that a predictable sequence of stimulations is expected. The theta band
 470 also showed cerebellar, inferior parietal cortex and SI activity for repeated stimulations relative to new
 471 stimulations.

472 **6 Acknowledgements**

473 The authors wish to thank Robert Oostenveld for valuable comments on an earlier version of the design.

474 Data for this study was collected at NatMEG (www.natmeg.se), the National infrastructure for
 475 Magnetoencephalography, Karolinska Institutet, Sweden. The NatMEG facility is supported by Knut & Alice
 476 Wallenberg (KAW2011.0207). The study, and Lau Møller Andersen, was funded by Knut & Alice Wallenberg
 477 Foundation (KAW2014.0102).

478 **7 References**

- Aleman, A., Böcker, K.B.E., Hijman, R., de Haan, E.H.F., Kahn, R.S., 2003. Cognitive basis of hallucinations in schizophrenia: role of top-down information processing. *Schizophr. Res.* 64, 175–185. [https://doi.org/10.1016/S0920-9964\(03\)00060-4](https://doi.org/10.1016/S0920-9964(03)00060-4)
- Alho, K., 1995. Cerebral Generators of Mismatch Negativity (MMN) and Its Magnetic Counterpart (MMNm) Elicited by Sound Changes. *Ear Hear.* 16, 38–51.
- Allen, M., Fardo, F., Dietz, M.J., Hillebrandt, H., Friston, K.J., Rees, G., Roepstorff, A., 2016. Anterior insula coordinates hierarchical processing of tactile mismatch responses. *NeuroImage* 127, 34–43. <https://doi.org/10.1016/j.neuroimage.2015.11.030>
- Arnfred, S.M., Eder, D.N., Hemmingsen, R.P., Glenthøj, B.Y., Chen, A.C.N., 2001. Gating of the vertex somatosensory and auditory evoked potential P50 and the correlation to skin conductance orienting response in healthy men. *Psychiatry Res.* 101, 221–235. [https://doi.org/10.1016/S0165-1781\(01\)00226-8](https://doi.org/10.1016/S0165-1781(01)00226-8)
- Attal, Y., Maess, B., Friederici, A., David, O., 2012. Head models and dynamic causal modeling of subcortical activity using magnetoencephalographic/electroencephalographic data. *Rev. Neurosci.* 23, 85–95. <https://doi.org/10.1515/rns.2011.056>
- Cheng, C.-H., Tsai, S.-Y., Liu, C.-Y., Niddam, D.M., 2017. Automatic inhibitory function in the human somatosensory and motor cortices: An MEG-MRS study. *Sci. Rep.* 7, 4234. <https://doi.org/10.1038/s41598-017-04564-1>
- Cheyne, D.O., 2013. MEG studies of sensorimotor rhythms: A review. *Exp. Neurol., Special Issue: Neuronal oscillations in movement disorders* 245, 27–39. <https://doi.org/10.1016/j.expneurol.2012.08.030>

- Coffey, E.B.J., Herholz, S.C., Chepesiuk, A.M.P., Baillet, S., Zatorre, R.J., 2016. Cortical contributions to the auditory frequency-following response revealed by MEG. *Nat. Commun.* 7, ncomms11070. <https://doi.org/10.1038/ncomms11070>
- Dale, A.M., Fischl, B., Sereno, M.I., 1999. Cortical surface-based analysis. I. Segmentation and surface reconstruction. *NeuroImage* 9, 179–94. <https://doi.org/10.1006/nimg.1998.0395>
- Dale, A.M., Liu, A.K., Fischl, B.R., Buckner, R.L., Belliveau, J.W., Lewine, J.D., Halgren, E., 2000. Dynamic Statistical Parametric Mapping: Combining fMRI and MEG for High-Resolution Imaging of Cortical Activity. *Neuron* 26, 55–67. [https://doi.org/10.1016/S0896-6273\(00\)81138-1](https://doi.org/10.1016/S0896-6273(00)81138-1)
- Engel, A.K., Fries, P., 2010. Beta-band oscillations—signalling the status quo? *Curr. Opin. Neurobiol., Cognitive neuroscience* 20, 156–165. <https://doi.org/10.1016/j.conb.2010.02.015>
- Fardo, F., Auzsztulewicz, R., Allen, M., Dietz, M.J., Roepstorff, A., Friston, K.J., 2017. Expectation violation and attention to pain jointly modulate neural gain in somatosensory cortex. *NeuroImage* 153, 109–121. <https://doi.org/10.1016/j.neuroimage.2017.03.041>
- Fischl, B., Sereno, M.I., Dale, A.M., 1999a. Cortical Surface-Based Analysis: II: Inflation, Flattening, and a Surface-Based Coordinate System. *NeuroImage* 9, 195–207. <https://doi.org/10.1006/nimg.1998.0396>
- Fischl, B., Sereno, M.I., Tootell, R.B.H., Dale, A.M., 1999b. High-resolution intersubject averaging and a coordinate system for the cortical surface. *Hum. Brain Mapp.* 8, 272–284. [https://doi.org/10.1002/\(SICI\)1097-0193\(1999\)8:4<272::AID-HBM10>3.0.CO;2-4](https://doi.org/10.1002/(SICI)1097-0193(1999)8:4<272::AID-HBM10>3.0.CO;2-4)
- Garrido, M.I., Barnes, G.R., Kumaran, D., Maguire, E.A., Dolan, R.J., 2015. Ventromedial prefrontal cortex drives hippocampal theta oscillations induced by mismatch computations. *NeuroImage* 120, 362–370. <https://doi.org/10.1016/j.neuroimage.2015.07.016>
- Giard, M.H., Lavikahen, J., Reinikainen, K., Perrin, F., Bertrand, O., Pernier, J., Näätänen, R., 1995. Separate Representation of Stimulus Frequency, Intensity, and Duration in Auditory Sensory Memory: An Event-Related Potential and Dipole-Model Analysis. *J. Cogn. Neurosci.* 7, 133–143. <https://doi.org/10.1162/jocn.1995.7.2.133>
- Gramfort, A., Luessi, M., Larson, E., Engemann, D.A., Strohmeier, D., Brodbeck, C., Goj, R., Jas, M., Brooks, T., Parkkonen, L., Hämäläinen, M., 2013. MEG and EEG data analysis with MNE-Python. *Brain Imaging Methods* 7, 267. <https://doi.org/10.3389/fnins.2013.00267>
- Gross, J., Kujala, J., Hämäläinen, M., Timmermann, L., Schnitzler, A., Salmelin, R., 2001. Dynamic imaging of coherent sources: Studying neural interactions in the human brain. *Proc. Natl. Acad. Sci.* 98, 694–699. <https://doi.org/10.1073/pnas.98.2.694>
- Hämäläinen, M.S., Hari, R., Ilmoniemi, R.J., Knuutila, J., Lounasmaa, O.V., 1993. Magnetoencephalography—theory, instrumentation, and applications to noninvasive studies of the working human brain. *Rev. Mod. Phys.* 65, 413–497. <https://doi.org/10.1103/RevModPhys.65.413>
- Hämäläinen, M.S., Ilmoniemi, R.J., 1994. Interpreting magnetic fields of the brain: minimum norm estimates. *Med. Biol. Eng. Comput.* 32, 35–42. <https://doi.org/10.1007/BF02512476>
- Hari, R., Forss, N., 1999. Magnetoencephalography in the study of human somatosensory cortical processing. *Philos. Trans. R. Soc. B Biol. Sci.* 354, 1145–1154. <https://doi.org/10.1098/rstb.1999.0470>
- Hari, R., Reinikainen, K., Kaukoranta, E., Hämäläinen, M., Ilmoniemi, R., Penttinen, A., Salminen, J., Teszner, D., 1984. Somatosensory evoked cerebral magnetic fields from SI and SII in man. *Electroencephalogr. Clin. Neurophysiol.* 57, 254–263. [https://doi.org/10.1016/0013-4694\(84\)90126-3](https://doi.org/10.1016/0013-4694(84)90126-3)
- Helmholtz, H. von, 1867. *Handbuch der physiologischen Optik.* Voss.
- Hillebrand, A., Barnes, G.R., 2002. A Quantitative Assessment of the Sensitivity of Whole-Head MEG to Activity in the Adult Human Cortex. *NeuroImage* 16, 638–650. <https://doi.org/10.1006/nimg.2002.1102>
- Holmes, C.J., Hoge, R., Collins, L., Woods, R., Toga, A.W., Evans, A.C., 1998. Enhancement of MR images using registration for signal averaging. *J. Comput. Assist. Tomogr.* 22, 324–333.
- Hsiao, F.-J., Cheng, C.-H., Chen, W.-T., Lin, Y.-Y., 2013. Neural correlates of somatosensory paired-pulse suppression: A MEG study using distributed source modeling and dynamic spectral power analysis. *NeuroImage* 72, 133–142. <https://doi.org/10.1016/j.neuroimage.2013.01.041>
- Kandel, E.R., Schwartz, J.H., Jessel, T.M., 2000. *Principles of Neural Science*, 4th ed. ed. McGraw-Hill, New York, NY, US.
- Karhu, J., Tesche, C.D., 1999. Simultaneous Early Processing of Sensory Input in Human Primary (SI) and Secondary (SII) Somatosensory Cortices. *J. Neurophysiol.* 81, 2017–2025.
- Lovero, K.L., Simmons, A.N., Aron, J.L., Paulus, M.P., 2009. Anterior insular cortex anticipates impending stimulus significance. *NeuroImage* 45, 976–983. <https://doi.org/10.1016/j.neuroimage.2008.12.070>
- Maris, E., Oostenveld, R., 2007. Nonparametric statistical testing of EEG- and MEG-data. *J. Neurosci. Methods* 164, 177–190.
- Mima, T., Nagamine, T., Nakamura, K., Shibasaki, H., 1998. Attention Modulates Both Primary and Second Somatosensory Cortical Activities in Humans: A Magnetoencephalographic Study. *J. Neurophysiol.* 80, 2215–2221. <https://doi.org/10.1152/jn.1998.80.4.2215>

- Näätänen, R., Gaillard, A.W.K., Mäntysalo, S., 1978. Early selective-attention effect on evoked potential reinterpreted. *Acta Psychol. (Amst.)* 42, 313–329. [https://doi.org/10.1016/0001-6918\(78\)90006-9](https://doi.org/10.1016/0001-6918(78)90006-9)
- Näätänen, R., Lehtokoski, A., Lennes, M., Cheour, M., Huottilainen, M., Iivonen, A., Vainio, M., Alku, P., Ilmoniemi, R.J., Luuk, A., Allik, J., Sinkkonen, J., Alho, K., 1997. Language-specific phoneme representations revealed by electric and magnetic brain responses. *Nature* 385, 432–434. <https://doi.org/10.1038/385432a0>
- Naeije, G., Vaulet, T., Wens, V., Marty, B., Goldman, S., Tiège, X.D., 2018. Neural Basis of Early Somatosensory Change Detection: A Magnetoencephalography Study. *Brain Topogr.* 31, 242–256. <https://doi.org/10.1007/s10548-017-0591-x>
- Niedermeyer, E., Silva, F.H.L. da, 2005. *Electroencephalography: Basic Principles, Clinical Applications, and Related Fields*. Lippincott Williams & Wilkins.
- Nyhus, E., Curran, T., 2010. Functional role of gamma and theta oscillations in episodic memory. *Neurosci. Biobehav. Rev., Binding Processes: Neurodynamics and Functional Role in Memory and Action* 34, 1023–1035. <https://doi.org/10.1016/j.neubiorev.2009.12.014>
- Oostenveld, R., Fries, P., Maris, E., Schoffelen, J.-M., 2011. FieldTrip: Open source software for advanced analysis of MEG, EEG, and invasive electrophysiological data. *Comput. Intell. Neurosci.* 2011, 156869. <https://doi.org/10.1155/2011/156869>
- Osipova, D., Takashima, A., Oostenveld, R., Fernández, G., Maris, E., Jensen, O., 2006. Theta and Gamma Oscillations Predict Encoding and Retrieval of Declarative Memory. *J. Neurosci.* 26, 7523–7531. <https://doi.org/10.1523/JNEUROSCI.1948-06.2006>
- Pazo-Alvarez, P., Cadaveira, F., Amenedo, E., 2003. MMN in the visual modality: a review. *Biol. Psychol.* 63, 199–236. [https://doi.org/10.1016/S0301-0511\(03\)00049-8](https://doi.org/10.1016/S0301-0511(03)00049-8)
- Pfurtscheller, G., Stancák, A., Neuper, C., 1996. Post-movement beta synchronization. A correlate of an idling motor area? *Electroencephalogr. Clin. Neurophysiol.* 98, 281–293. [https://doi.org/10.1016/0013-4694\(95\)00258-8](https://doi.org/10.1016/0013-4694(95)00258-8)
- Roux, F., Uhlhaas, P.J., 2014. Working memory and neural oscillations: alpha–gamma versus theta–gamma codes for distinct WM information? *Trends Cogn. Sci.* 18, 16–25. <https://doi.org/10.1016/j.tics.2013.10.010>
- Salmelin, R., Hämäläinen, M., Kajola, M., Hari, R., 1995. Functional Segregation of Movement-Related Rhythmic Activity in the Human Brain. *NeuroImage* 2, 237–243. <https://doi.org/10.1006/nimg.1995.1031>
- Salmelin, R., Hari, R., 1994. Spatiotemporal characteristics of sensorimotor neuromagnetic rhythms related to thumb movement. *Neuroscience* 60, 537–550. [https://doi.org/10.1016/0306-4522\(94\)90263-1](https://doi.org/10.1016/0306-4522(94)90263-1)
- Schack, B., Vath, N., Petsche, H., Geissler, H.-G., Möller, E., 2002. Phase-coupling of theta–gamma EEG rhythms during short-term memory processing. *Int. J. Psychophysiol.* 44, 143–163. [https://doi.org/10.1016/S0167-8760\(01\)00199-4](https://doi.org/10.1016/S0167-8760(01)00199-4)
- Swerdlow, N.R., Caine, S.B., Braff, D.L., Geyer, M.A., 1992. The neural substrates of sensorimotor gating of the startle reflex: a review of recent findings and their implications. *J. Psychopharmacol. (Oxf.)* 6, 176–190. <https://doi.org/10.1177/026988119200600210>
- Taulu, S., Simola, J., 2006. Spatiotemporal signal space separation method for rejecting nearby interference in MEG measurements. *Phys. Med. Biol.* 51, 1759–1768. <https://doi.org/10.1088/0031-9155/51/7/008>
- Tenney, J.R., Fujiwara, H., Horn, P.S., Jacobson, S.E., Glauser, T.A., Rose, D.F., 2013. Focal corticothalamic sources during generalized absence seizures: A MEG study. *Epilepsy Res.* 106, 113–122. <https://doi.org/10.1016/j.eplepsyres.2013.05.006>
- Tesche, C.D., Karhu, J., 1997. Somatosensory evoked magnetic fields arising from sources in the human cerebellum. *Brain Res.* 744, 23–31. [https://doi.org/10.1016/S0006-8993\(96\)01027-X](https://doi.org/10.1016/S0006-8993(96)01027-X)
- Tesche, C.D., Karhu, J.J.T., 2000. Anticipatory cerebellar responses during somatosensory omission in man. *Hum. Brain Mapp.* 9, 119–142. [https://doi.org/10.1002/\(SICI\)1097-0193\(200003\)9:3<119::AID-HBM2>3.0.CO;2-R](https://doi.org/10.1002/(SICI)1097-0193(200003)9:3<119::AID-HBM2>3.0.CO;2-R)
- Teufel, C., 2018. Sensory Neuroscience: Linking Dopamine, Expectation, and Hallucinations. *Curr. Biol.* 28, R158–R160. <https://doi.org/10.1016/j.cub.2018.01.003>
- Tzourio-Mazoyer, N., Landeau, B., Papathanassiou, D., Crivello, F., Etard, O., Delcroix, N., Mazoyer, B., Joliot, M., 2002. Automated Anatomical Labeling of Activations in SPM Using a Macroscopic Anatomical Parcellation of the MNI MRI Single-Subject Brain. *NeuroImage* 15, 273–289. <https://doi.org/10.1006/nimg.2001.0978>
- van Ede, F., Jensen, O., Maris, E., 2010. Tactile expectation modulates pre-stimulus β -band oscillations in human sensorimotor cortex. *NeuroImage* 51, 867–876. <https://doi.org/10.1016/j.neuroimage.2010.02.053>
- van Ede, F., Lange, F. de, Jensen, O., Maris, E., 2011. Orienting Attention to an Upcoming Tactile Event Involves a Spatially and Temporally Specific Modulation of Sensorimotor Alpha- and Beta-Band Oscillations. *J. Neurosci.* 31, 2016–2024. <https://doi.org/10.1523/JNEUROSCI.5630-10.2011>
- Yabe, H., Tervaniemi, M., Reinikainen, K., Näätänen, R., 1997. Temporal window of integration revealed by MMN to sound omission. *Neuroreport* 8, 1971–1974.